Free Energy Cost of Reducing Noise while Maintaining a High Sensitivity

Pablo Sartori[1,*] and Yuhai Tu[2]
[1]Max Planck Institute for the Physics of Complex Systems, Noethnitzer Strasse 38, 01187 Dresden, Germany
[2]IBM T.J. Watson Research Center, 1101 Kitchawan Road, Yorktown Heights, New York 10598, USA
(Received 27 May 2015; published 8 September 2015)

Living systems need to be highly responsive, and also to keep fluctuations low. These goals are incompatible in equilibrium systems due to the fluctuation dissipation theorem (FDT). Here, we show that biological sensory systems, driven far from equilibrium by free energy consumption, can reduce their intrinsic fluctuations while maintaining high responsiveness. By developing a continuum theory of the *E. coli* chemotaxis pathway, we demonstrate that adaptation can be understood as a nonequilibrium phase transition controlled by free energy dissipation, and it is characterized by a breaking of the FDT. We show that the maximum response at short time is enhanced by free energy dissipation. At the same time, the low frequency fluctuations and the adaptation error decrease with the free energy dissipation algebraically and exponentially, respectively.

DOI: 10.1103/PhysRevLett.115.118102 PACS numbers: 87.18.Tt, 05.70.Ln, 87.10.Vg

Living organisms need to respond to external signals with high sensitivity, and at the same time, they also need to control their internal fluctuations in the absence of signal. In equilibrium systems, the fluctuation dissipation theorem (FDT) dictates that these two desirable properties, high sensitivity and low fluctuation, cannot be satisfied simultaneously. Most sensory and regulatory functions in biology are carried out by biochemical networks that operate out of equilibrium—metabolic energy is spent to drive the dynamics of the network [1–4]. Thus, in principle, they are not constrained by the FDT [5]. How fluctuations, energy dissipation, and sensitivity are related for such systems remains not well understood. Here, we address this question by studying a negative feedback network responsible for adaptation in the bacterial chemosensory system [6–9].

A typical adaptive behavior in a small system such as a single cell is shown in Fig. 1(a) [10]. In response to a change of the signal S, the output y of the sensory system first changes quickly with a fast time scale τ_y. After the fast response, the output slowly adapts back towards its prestimulus level $a_{\rm ad}$ with an adaptation time $\tau_{\rm ad} \gg \tau_y$. The new steady state (adapted) output may differ from the prestimulus value, and the difference is quantified by the adaptation error ϵ. In our previous work [11], we showed that the negative feedback network responsible for adaptation operates out of equilibrium with a finite free energy dissipation rate $\dot{W}$. The average adaptation error $\langle\epsilon\rangle$ was found to decrease exponentially with $\tau_{\rm ad}\dot{W}$. However, how the variance σ_ϵ^2 of the error behaves in an adaptive system still remains unknown. This is an important question as adaptive feedback systems are intrinsically noisy due to the slow adaptation dynamics [12].

In the linear response regime, the output response of a system to an input signal $S(t)$ is given by $R(t) = R(0) + \int_0^t \chi(t-t')S(t')dt'$, where χ is the response function. For equilibrium systems, under the general assumption that response and signal are conjugate variables, the FDT establishes that $\chi(t) = -\beta\partial_t C_R(t)\Theta(t)$, where $C_R(t) \equiv \langle R(t)R(0)\rangle - \langle R\rangle^2$ is the autocorrelation function, $\Theta(t)$ is the Heaviside function, and $\beta = (k_{\rm B}T)^{-1}$ is the inverse thermal energy set to unity hereafter. For a small step stimulus $S(t) = S_0\Theta(t)$, integration of the FDT leads to a relation between the response and its correlation: $R(t) = R(0) - S_0[C_R(t) - C_R(0)]$. Since for systems in chemical equilibrium $C_R(t)$ is a monotonically decreasing function of time [13], the response $R(t)$ is also monotonic in time, and thus no adaptation dynamics is possible. Furthermore, the long time response $\Delta R \equiv R(t=\infty) - R(0)$ is linearly proportional to the variance $\sigma_R^2 = C_R(0)$, i.e., $\Delta R = S_0\sigma_R^2$.

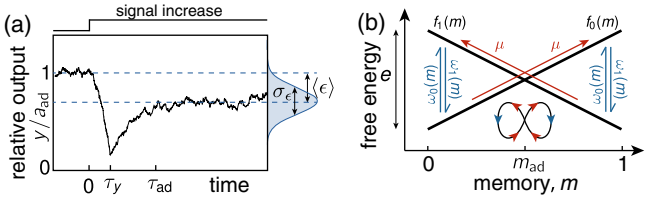

FIG. 1 (color online). Noisy response of feedback adaptation. (a) Adaptive output response to a step input signal increase at time 0. After a sharp decrease in a time τ_y, the output y recovers back in a time $\tau_{\rm ad}$ to its adapted value $a_{\rm ad}$. The adaptation error is characterized by its average $\langle\epsilon\rangle$, as well as its variance σ_ϵ. (b) Schematic of the feedback adaptation model. Transitions between the active and inactive memory energy landscapes, f_1 and f_0, are mediated via equilibrium activity transitions with rates ω_0 and ω_1. An external chemical energy input μ is used to drive the memory variable uphill in both the active and inactive states. The result is a dissipative loop of probability flow around the adapted memory state $m_{\rm ad}$, which ensures the output to be near $a_{\rm ad}$.

In this Letter, we show that in a nonequilibrium adaptive system both the average adaptation error $\langle\epsilon\rangle$ (analogous to ΔR) and its variance σ_ϵ^2 (analogous to σ_R^2) are suppressed by the free energy dissipation of the system but in different ways, which results in a nonlinear (logarithmic) relationship between them. More importantly, violation of the FDT allows suppression of noise without compromising the strength of the short time response.

The continuous model of feedback adaptation.—We start by introducing a discrete adaptation model motivated by the *E. coli* chemotaxis pathway. The system is characterized by its binary receptor activity $A = 0, 1$, its output y, and an internal control variable $M = 0, 1, \ldots, N$, that corresponds to the chemoreceptor's methylation level in *E. coli* chemotaxis [9]. For a given external input signal S, the free energy of the system can be written as

$$F_A(M, S) = -(A - 1/2)[(M - M_r)E - (S - S_r)], \quad (1)$$

where S_r is a reference signal at a methylation level M_r, and E (which is positive) sets the methylation energy scale. For *E. coli* chemotaxis, the signal S depends on the ligand attractant concentration logarithmically [14].

The dynamics of the system is characterized by the transitions among the $2 \times (N + 1)$ states in the $A \times M$ phase space. The receptor activity switches at a time scale τ_a, which is much shorter than the adaptation time scale $\tau_{\rm ad}$ at which the internal variable M is controlled. The activity A determines the output y of the signaling pathway. In the case of *E. coli* chemotaxis, this is carried out by the phosphorylation and dephosphorylation reactions of the response regulator CheY with an intermediate time scale τ_y: $\tau_{\rm ad} \gg \tau_y \gg \tau_a$. To account for this, we express y by $y(t) = \tau_y^{-1} \int_{-\infty}^{t} e^{(t'-t)/\tau_y} A(t') dt'$, which averages the fast binary activity A over the time scale τ_y.

According to Eq. (1), a larger signal S favors the inactive state $A = 0$. Thus, an increase in S quickly reduces the system's average activity, at time scale $\sim\tau_a$, and output, at time scale $\sim\tau_y$, as represented in Fig. 1(a). After this sudden initial response, the system slowly adapts by adjusting its internal variable M to balance the effect of the increased signal. Because of its slow time scale, M effectively serves as a memory of the system. This adaptation process restores activity and output to a level near their prestimulus value $\langle A\rangle = \langle y\rangle \approx a_{\rm ad}$. Although highly precise, adaptation is imperfect, and its inaccuracies are quantified by the adaptation error ϵ, which we define as

$$\epsilon = \frac{y - a_{\rm ad}}{a_{\rm ad}}. \quad (2)$$

For *E. coli* chemotaxis, the adaptive machinery consists of chemical reactions that increase M in the inactive state and decrease it in the active state. Note from Eq. (1) that such regulatory reactions are energetically unfavorable, and thus require a chemical driving force μ; see Fig. 1(b).

To gain analytical insights about dynamics and energetics of adaptation, we consider the limit where $N \to \infty$ and $m = M/N \in [0, 1]$ becomes a continuous variable [15]. Note that free energy and bare rates need to be rescaled for the continuum limit to converge (see Supplemental Material [16] for details). Proceeding in this way we obtain two coupled Fokker-Planck equations that describe the chemotaxis pathway dynamics:

$$\begin{aligned} \partial_t p_1 &= p_0\omega_0 - p_1\omega_1 - \partial_m J_1, \\ \partial_t p_0 &= p_1\omega_1 - p_0\omega_0 - \partial_m J_0, \end{aligned} \quad (3)$$

where $p_1(m, t)$ and $p_0(m, t)$ are the probabilities of m for the active and inactive states, respectively. The probability currents are given by

$$J_A = D_A(-[\partial_m f_A + (A - 1/2)\mu]p_A - \partial_m p_A), \quad (4)$$

for $A = 0, 1$, and where $f_A(m) = -(A - 1/2)[(m - m_r)e - (S - S_r)]$ is the continuum limit of Eq. (1) characterized by the rescaled energy parameter $e = NE$. The fast transition rates between the active and inactive states, ω_0 and ω_1, satisfy detailed balance $\omega_0/\omega_1 = \exp(f_0 - f_1)$. The diffusionlike constants D_1 and D_0 set the time scale of m changes for active and inactive states, and thus the adaptation time goes as $\tau_{\rm ad} \sim D_A^{-1}$ and is independent of μ, see Supplemental Material [16]. Our model is analogous to that of an isothermal ratchet [17], where a chemical driving fuels directed motion. Whereas in ratchets μ drives directed motion, here it fuels currents up the energy landscapes f_0 and f_1 to achieve adaptation.

In the absence of external driving, i.e., $\mu = 0$, the system relaxes to a state of thermal equilibrium with no phase-space fluxes $J_0 = J_1 = 0$. In this regime adaptation is impossible. The chemical driving $\mu > 0$ breaks detailed balance and creates currents that increase m in the inactive state and decrease it in the active state. For large enough μ, the memory variable m can be stabilized (trapped) in a cycle around its adapted state $m_{\rm ad}$, which ensures $\langle y\rangle \approx a_{\rm ad}$ as illustrated in Fig. 1(b). The free energy dissipation rate of this process, $\dot{W}$, can be computed, and is given by $\dot{W} \approx C|\mu|/\tau_{\rm ad}$, with C a system specific constant set to unity by our parameter choice; see the Supplemental Material [16]. In the following, we will use the chemical driving $\mu \approx \tau_{\rm ad}\dot{W}$ to characterize the system's energy dissipation.

The dynamics of A, y, and m are illustrated in Fig. 2(a). The power spectra of A and y, given in Fig. 2(b), show that the high frequency fluctuation of y is suppressed with respect to that of A by time averaging. However, the low frequency fluctuations of y, which are caused by the slow fluctuations of m, are not affected. These slow fluctuations, which can affect the bacterium's swimming behavior due to

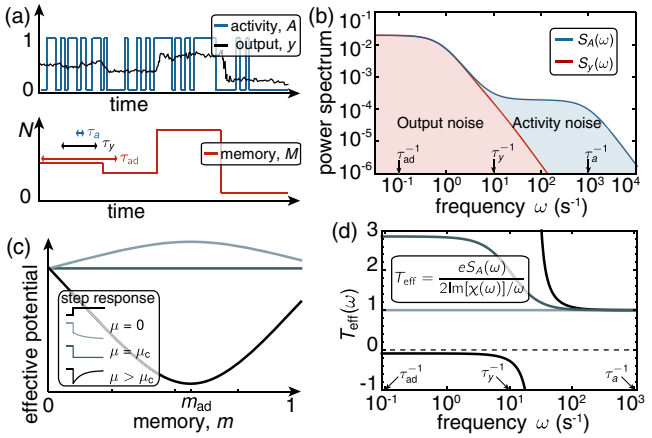

FIG. 2 (color online). Adaptation as a nonequilibrium transition. (a) Schematic time traces of the binary activity A (blue), the output y (black), and the memory M (red) in steady state. The slow M variations induce large fluctuations in the output y, while the fast A switching for a fixed M only produces small fluctuations in y. (b) Power spectra of the activity S_A and output S_y. The output noise is filtered (reduced) in the high frequency range $\tau_y^{-1} < \omega < \tau_a^{-1}$, but it remains unfiltered in the range $\tau_{\rm ad}^{-1} < \omega < \tau_y^{-1}$. (c) Effective memory potential in Eq. (5) for three values of the chemical driving μ (due to the choice $D_1 = D_0$ taken here, $m_{\rm ad} = m_*$). At equilibrium, $\mu = 0$, the adapted memory state $m_{\rm ad}$ is unstable. At the value $\mu = \mu_{\rm c}$ the system becomes critical. In the region $\mu > \mu_{\rm c}$ the adapted state $m_{\rm ad}$ is stable, and the system adapts output and activity to $a(m_{\rm ad})$. Inset: Activity response to step signal increase for corresponding values of μ. (d) Effective temperature $T_{\rm eff}$ for three different values of the chemical driving μ. After the onset of adaptation a region with "negative friction" develops, at the end of which the effective temperature diverges. Values of μ from lighter to darker blue are $\mu = 0$, $\mu = 0.65\mu_{\rm c}$, and $\mu = 20\mu_{\rm c}$ [the same as in panel (c)]. The other parameters are from Ref. [18]; see the Supplemental Material [16].

the motor's ultrasensitivity, are suppressed by free energy dissipation, as we show later in this Letter.

Adaptation as a nonequilibrium phase transition.—Given the separation of time scales $\tau_a \ll \tau_{\rm ad}$, we can solve Eqs. (3) by using the adiabatic approximation [13,18]: $p_1(m) = a(m)p(m)$, and $p_0(m) = [1 - a(m)]p(m)$, with $a(m) = (1 + e^{f_1(m) - f_0(m)})^{-1}$ the average equilibrated activity for a fixed value of m. The distribution of m can be written as $p(m) = e^{-h(m,S)}/Z$ with h the effective potential and Z a normalization constant. We have determined the effective potential h analytically (see Supplemental Material [16]):

$$h(m,S) = \frac{\mu}{\mu_{\rm c}} \ln[D_0 e^{-(m-m_*)e/2} + D_1 e^{(m-m_*)e/2}] - \ln[e^{-(m-m_*)e/2} + e^{(m-m_*)e/2}], \quad (5)$$

where we have defined the critical chemical driving as $\mu_{\rm c} = e/2$, and $m_* = m_{\rm r} + (S - S_{\rm r})/e$.

The analytical form of the effective potential is one of the main results of this Letter. The effect of energy dissipation and the onset of adaptation can be understood intuitively with $h(m,S)$, which contains two terms with similar shapes; see Fig. 2(c). The first term (proportional to $\mu/\mu_{\rm c}$) in the right-hand side of Eq. (5) comes from chemical driving (nonequilibrium effect) and has a stable free energy minimum. The second term is the equilibrium potential in the absence of driving, and has a maximum at m_*. At equilibrium the only critical point m_* is unstable, so the system tends to go to the boundaries without adapting. As μ increases and opposes the force generated by f_A the first part of the potential starts to dominate. For $\mu > \mu_{\rm c}$, the system develops a stable fixed point at $m_{\rm ad}$ indicating the onset of adaptive behaviors towards $a(m_{\rm ad})$ [19]. As μ grows it dominates the slope of h near the fixed point increasing its stability, and adaptation accuracy improves. The transition of a feedback system to adaptation can thus be loosely understood as a continuous phase transition (see the Supplemental Material [16]). Since the control parameter is the free energy dissipation, the transition to adaptation occurs far from equilibrium and a breaking of FDT is to be expected.

Breakdown of fluctuation dissipation theorem.—In our feedback model, the observable conjugate to the signal is $eA = -\partial_S f_A$, something that does not hold for feedforward models where the adaptive machinery can be maintained at no energy cost [20–22]. At equilibrium the FDT leads then to $\chi(t) = e\partial_t C_A(t)$, where χ is the activity response function and C_A the monotonic correlation function. In an adaptive system the integral of χ, which is just the response to a step stimulus, is nonmonotonic; therefore, FDT is broken and adaptation occurs out of equilibrium.

To quantify the departure from equilibrium, we define an effective temperature $T_{\rm eff}$ using the formulation of the FDT in frequency space [5,23]; see inset in Fig. 2(d). The frequency dependence of $T_{\rm eff}$ for $\mu > 0$ implies a breakdown of FDT. As shown in Fig. 2(d), while for any value $\mu \neq 0$ we have $T_{\rm eff} \neq 1$, after the transition to the adaptive regime $\mu \geq \mu_{\rm c}$ a divergence occurs. This corresponds to the appearance of a frequency region where $\mathrm{Im}[\chi(\omega)] < 0$. A negative effective viscosity indicates the dominance of the active effects that drive a net current to flow against the gradients of the equilibrium energy landscapes (f_A), which was also observed in other biological systems such as collections of motors [24] or the inner ear hair bundle [5]. The breakdown of FDT means that there is no *a priori* connection among fluctuations σ_ϵ^2, chemical driving μ (dissipation), and long-time response $\langle\epsilon\rangle$. In the following we derive relations linking these three quantities in the adaptive feedback system studied here.

The free energy cost of suppressing fluctuations.—As evident from the effective potential, increasing the chemical driving μ stabilizes the adapted state. In the limit $\mu \to \infty$, the system thus goes to its perfectly adapted state with

average activity and output $a_{\rm ad} = D_0/(D_0 + D_1)$, that is $a(m_{\rm ad}) \to a_{\rm ad}$. For finite μ, the output differs from $a_{\rm ad}$, which can be characterized by the average error $\langle\epsilon\rangle$ and its variance σ_ϵ^2.

The average adaptation error is $\langle\epsilon\rangle = (\langle y\rangle - a_{\rm ad})/a_{\rm ad}$. Summing and integrating Eqs. (3) at the steady state, we have

$$\langle\epsilon\rangle = \frac{D_1 p_1(1) + D_0 p_0(1)}{D_0(e/2-\mu)} - \frac{D_1 p_1(0) + D_0 p_0(0)}{D_0(e/2-\mu)}. \quad (6)$$

Thus to obtain the adaptation error we only need to evaluate the probability at the boundaries. In the limit of $\mu \gg \mu_{\rm c}$, we have

$$\langle\epsilon\rangle \approx \epsilon_{\rm c} e^{-k\mu\mu_{\rm c}}, \quad (7)$$

where k and $\epsilon_{\rm c}$ are constants with only weak dependence on μ and S (see Supplemental Material [16]). This shows explicitly that the adaptation error goes down exponentially with energy dissipation, as found numerically in our previous work for the discrete model [11]. Here, we show this relationship analytically in the continuum limit, which is consistent with direct simulations of the discrete model; see Fig. 3(a).

Besides stabilizing the adapted state, Eq. (5) shows that increasing μ also reduces the m fluctuations by making the effective potential sharper. The reduction in these fluctuations implies a decrease in the variance of the error σ_ϵ^2. Taking into account the separation of time scales, the variance of the output y can be approximated as the sum of two variances σ_{ym}^2 and σ_a^2. They, respectively, correspond to variation of y at time scale $\sim\tau_y$ around its average $a(m)$ for a fixed m, and the variation of $a(m)$ due to variation of m at the adaptation time $\sim\tau_{\rm ad}$; see Fig. 2(a). We thus have

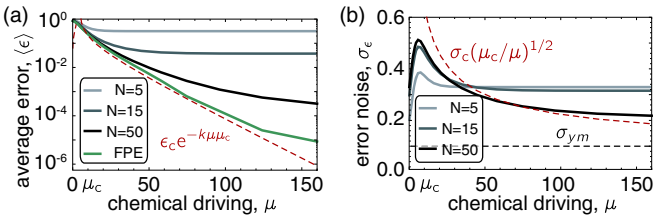

FIG. 3 (color online). Free energy cost of reducing error and noise. (a) Dependence of average error with chemical driving for several system sizes. The decay is exponential, in agreement with the infinite size limit (dashed red). Saturation of the decay for finite N is due to finite size effects. (b) Adaptation noise as a function of chemical driving for several system sizes, together with the analytical estimate in dashed red. At very large driving the noise saturates to its minimum σ_{ym} dictated by the intrinsic activity fluctuations. Note that at the critical driving $\mu_{\rm c}$ the analytical estimate diverges. This divergence is smoothed for finite N.

$$\sigma_\epsilon^2 \approx (\sigma_{ym}^2 + \sigma_a^2)/a_{\rm ad}^2. \quad (8)$$

The variance σ_{ym}^2 of y is caused by the fast fluctuations of the binary variable A at time scale $\sim\tau_a$ averaged over the output time scale $\tau_y \gg \tau_a$ (see Supplemental Material [16]):

$$\sigma_{ym}^2 = (a_{\rm ad} - a_{\rm ad}^2)\tau_a/(\tau_y + \tau_a),$$

which clearly shows that $\sigma_{ym}^2 \propto \tau_a/\tau_y$ is reduced by time averaging [12,25].

The variance $\sigma_a^2 = \langle a^2\rangle - \langle a\rangle^2$, where $\langle a^n\rangle = \int_0^1 a^n(m)p(m)dm$ for $n = 1, 2$, is caused by the slow variation of m, and cannot be reduced by time average. To obtain an analytical expression for σ_a^2 we approximate $p(m)$ by a Gaussian, valid for $\mu \gg \mu_{\rm c}$. This results in $\sigma_a^2 \approx (\partial_m a_{\rm ad})^2\sigma_m^2$. The variance $\sigma_m^2 = \langle m^2\rangle - \langle m\rangle^2$ within the same Gaussian approximation of $p(m)$ is given by $\sigma_m^2 \approx (\mu\mu_{\rm c})^{-1}$. Defining now a characteristic variance as $\sigma_c^2 = (1 - a_{\rm ad})^2 a_{\rm ad}^2$, we finally have

$$\sigma_a^2 \approx \sigma_c^2\mu_{\rm c}/\mu, \quad (9)$$

which vanishes when $\mu \to \infty$. This is a main result of the Letter, which shows that energy dissipation is used to reduce error noise by suppressing slow activity fluctuations. This result is verified by direct simulations of the discrete models with increasing N; see Fig. 3(b).

Discussion.—Biochemical networks are nonequilibrium systems fueled by free energy dissipation to achieve their biological functions. Energy dissipation liberates the networks from constraints such as the fluctuation dissipation theorem and detailed balance. Here, we show in a negative feedback network that the long-time output response $\Delta\langle y\rangle = a_{\rm ad}\langle\epsilon\rangle$ decreases with the free energy dissipation $\mu \approx \tau_{\rm ad}\dot{W}$ exponentially, and its fluctuation $\sigma_y^2 = a_{\rm ad}^2\sigma_\epsilon^2$ decreases as μ^{-1}, making the latter a limiting factor for accuracy at large μ. These effects, which arise from an improved accuracy and smaller fluctuations of the adaptation dynamics, contribute to enhance the short time response $\langle y\rangle_{\rm max}$; see Fig. 4.

Even though FDT is broken in the adaptive system studied here, fluctuations and long-time response of the output are linked via a nonlinear relation: $\sigma_y^2 \approx d\mu_{\rm c}^2/\ln(y_{\rm c}/\Delta\langle y\rangle) + \sigma_{ym}^2$, where $d = k\sigma_{\rm c}^2$ and $y_c = a_{\rm ad}\epsilon_{\rm c}$. Unlike the linear nonequilibrium FDT derived by a change of observables [26–28], our nonlinear relation links observables that are conjugate at equilibrium, making it particularly appealing. Our work is closely related to the bound derived in Ref. [29] for fluctuations of currents and in Ref. [30] for reduction in concentration estimates. We expect that the results here shown are generically applicable to feedback adaptive systems. And, while there is evidence that their scope could be broader [31], it remains a challenging question to formulate a general relationship

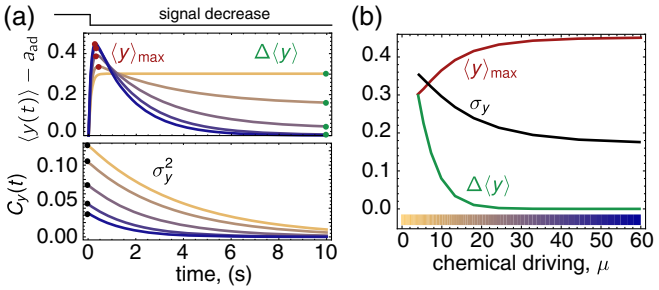

FIG. 4 (color online). Response and correlations in systems out of equilibrium. (a) (top panel) Average output response to a signal decrease for several values of the chemical driving beyond μ_c, see the color code for μ in panel (b). As the chemical driving μ increases, the maximal transient response $\langle y\rangle_{max}$ increases, but the long time response $\Delta\langle y\rangle = a_{ad}\langle\epsilon\rangle$ decreases. (bottom panel) The correlation function also decreases as the system is driven further away from equilibrium. (b) The dependence of $\langle y\rangle_{max}$, $\Delta\langle y\rangle$, and σ_y on the chemical driving μ. The long-time response (adaptation error) $\Delta\langle y\rangle$ decreases quickly with μ. The output fluctuation σ_y, dominated by the memory noise σ_m, decays more gradually with μ, and controls the increase in the maximal response $\langle y\rangle_{max}$ for large μ. In this figure $N = 15$, and $S = S_r$.

among response, fluctuations, and energy dissipation for systems far from equilibrium.

This work is partly supported by a NIH Grant (No. R01GM081747 to Y. T.). We thank Leo Granger and Jordan Horowitz for a critical reading of this manuscript, and four anonymous referees for a thorough and constructive criticism of this work.

*pablosv@pks.mpg.de

[1] H. Qian, Annu. Rev. Phys. Chem. **58**, 113 (2007).
[2] P. Mehta and D. J. Schwab, Proc. Natl. Acad. Sci. U.S.A. **109**, 17978 (2012).
[3] J. E. Niven and S. B. Laughlin, J. Exp. Biol. **211**, 1792 (2008).
[4] C. H. Bennett, BioSystems **11**, 85 (1979).
[5] P. Martin, A. Hudspeth, and F. Jülicher, Proc. Natl. Acad. Sci. U.S.A. **98**, 14380 (2001).
[6] H. C. Berg and D. A. Brown, Nature (London) **239**, 500 (1972).
[7] S. M. Block, J. E. Segall, and H. C. Berg, J. Bacteriol. **154**, 312 (1983).
[8] N. Barkai and S. Leibler, Nature (London) **387**, 913 (1997).
[9] Y. Tu, Annu. Rev. Biophys. **42**, 337 (2013).
[10] D. E. Koshland, A. Goldbeter, and J. B. Stock, Science **217**, 220 (1982).
[11] G. Lan, P. Sartori, S. Neumann, V. Sourjik, and Y. Tu, Nat. Phys. **8**, 422 (2012).
[12] P. Sartori and Y. Tu, J. Stat. Phys. **142**, 1206 (2011).
[13] N. G. Van Kampen, 3rd ed. *Stochastic Processes in Physics and Chemistry* (Elsevier Ltd., New York, 2007).
[14] Y. Kalinin, L. Jiang, Y. Tu, and M. Wu, Biophys. J. **96**, 2439 (2009).
[15] C. W. Gardiner, *Handbook of Stochastic Methods for Physics, Chemistry, and the Natural Sciences* (Springer, Berlin, 2004), Vol. 4.
[16] See Supplemental Material at http://link.aps.org/supplemental/10.1103/PhysRevLett.115.118102 for details in derivations.
[17] A. Parmeggiani, F. Jülicher, A. Ajdari, and J. Prost, Phys. Rev. E **60**, 2127 (1999).
[18] Y. Tu, T. S. Shimizu, and H. C. Berg, Proc. Natl. Acad. Sci. U.S.A. **105**, 14855 (2008).
[19] A. E. Allahverdyan and Q. A. Wang, Phys. Rev. E **87**, 032139 (2013).
[20] W. Buijsman and M. Sheinman, Phys. Rev. E **89**, 022712 (2014).
[21] G. De Palo and R. G. Endres, PLoS Comput. Biol. **9**, e1003300 (2013).
[22] P. Sartori, L. Granger, C. F. Lee, and J. M. Horowitz, PLoS Comput. Biol. **10**, e1003974 (2014).
[23] L. F. Cugliandolo, J. Kurchan, and L. Peliti, Phys. Rev. E **55**, 3898 (1997).
[24] F. Jülicher and J. Prost, Phys. Rev. Lett. **78**, 4510 (1997).
[25] H. C. Berg and E. M. Purcell, Biophys. J. **20**, 193 (1977).
[26] D. Bedeaux, S. Milosevic, and G. Paul, J. Stat. Phys. **3**, 39 (1971).
[27] J. Prost, J.-F. Joanny, and J. M. R. Parrondo, Phys. Rev. Lett. **103**, 090601 (2009).
[28] U. Seifert and T. Speck, Europhys. Lett. **89**, 10007 (2010).
[29] A. C. Barato and U. Seifert, Phys. Rev. Lett. **114**, 158101 (2015).
[30] C. C. Govern and P. R. ten Wolde, Phys. Rev. Lett. **113**, 258102 (2014).
[31] Y. Cao, H. Wang, Q. Ouyang, and Y. Tu, Nat. Phys. **11**, 772 (2015).